# Lamellar Mesophases in Polyacrylonitrile: A Synchrotron Small-Angle X-ray Scattering Study

**Andreas F. Thünemann***

*Max Planck Institute of Colloids & Interfaces, Am Mühlenberg, 14476 Golm, Germany*

**W. Ruland**

*Fachbereich Chemie und Zentrum für Materialwissenschaften, Philipps-Universität Marburg, Germany*

*Received August 4, 1999; Revised Manuscript Received January 20, 2000*

ABSTRACT: The formation of lamellar structures in polyacrylonitrile (PAN) fibers was investigated in the temperature range from 25 to 500 °C using synchrotron small-angle X-ray scattering. It was found that, in addition to a first lamellar mesophase showing up at about 200−300 °C, a second lamellar mesophase appears in an inert atmosphere at temperatures higher than about 350 °C. The former was attributed to the cyclization, the latter to the aromatization reaction of PAN. The periods of the first (α) and the second (*β*) lamellar phase are about 13 and 5 nm, respectively. Both the α and the *β* phase show preferred orientation. The average angle between the fiber axis and the normals of the lamellae is about 15°. Homopolymer and copolymer fibers differ considerably in the kinetics of developing the α phase.

## 1. Introduction

Polyacrylonitrile fibers are used widely for textiles and as reinforcement fibers. The pyrolysis of PAN fibers results in black orlon, a dark and noninflammable product. This represents the first stage in the formation of carbon fibers and is an important industrial process consisting of a number of chemical reactions and structural reorganizations. Reviews on the thermal conversation of PAN have been given by Wöhrle,[1] Olivé and Olivé,[2] Jain and Abhiraman,[3,4] Jain et al.,[4] and Bashir.[5] A simplified reaction scheme is given in Figure 1. The conversation of PAN fibers to carbon fibers starts with an exothermic cyclization reaction in the range of 200−300 °C during which adjacent nitrile groups form conjugated CN sequences. The conjugated sequences are restricted to a length of about three to six rings. At the end of the cyclization reaction, about 20% of the nitrile groups remain unchanged. At a temperature of about 360 °C, the dehydration of the fibers to a polymer with naphthiridine moieties begins. These planar ladder chains cross-link to form a two-dimensional network at temperatures in the range from 400 to 700 °C. During the aromatization, hydrogen- and nitrogen-rich fragments split off and extensive polymer structures with $sp^2$ carbon atoms are formed. The nitrogen content decreases from 26% (PAN fibers) to 2−5% (carbon fibers).

The appearance of a lamellar structure during the first stages of the heat treatment of PAN fibers has been reported by Tyson,[6] Fillery and Goodhew,[7] Hinrichsen,[8] Warner,[9] Warner et al.,[10] and Walenta and Fink.[11] It was assumed that the formation of the lamellar structure on heating is due to ordered and disordered domains already present in the pristine fibers, similar to the effect observed in the rayon fibers.[12] However, detailed X-ray studies on the structure of PAN fibers carried out recently[14] have shown that PAN fibers have a uniform pseudohexagonal structure and that, in particular, a semicrystalline structure can be excluded. This observation is corroborated by the fact that pristine fibers do not show any meridional synchrotron small-angle X-ray scattering (SAXS) maxima.

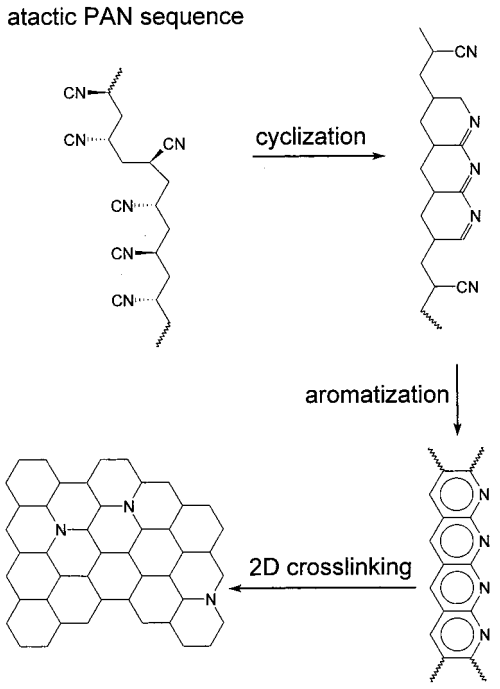


**Figure 1.** Schematic representation of the reaction stages during the thermal transformation of PAN to carbon fibers.

The aim of the present work is to obtain more information on the lamellar structure and its formation using time- and temperature-dependent synchrotron SAXS.

## 2. Theoretical Section

The following treatment uses largely the symbols already defined in earlier publications.[15−17] We consider the 2D SAXS intensity distribution obtained with

* Corresponding author. E-mail: andreas@mpikg-golm.mpg.de.

10.1021/ma991298k CCC: $19.00 
Published on Web 03/08/2000

pinhole collimation, containing the scattering of lamellar structures and elongated microvoids, both with preferred orientation. The contribution of density fluctuations and the effect of the finite width of the domain boundaries are supposed to be eliminated.

**2.1. Lamellar Structures.** The scattering intensity $I$ of an ensemble of lamellar structures with uniaxial preferred orientation is given by

$$I(\mathbf{s}) = \sum_i I_l(\mathbf{T}_i\mathbf{s})$$

where $\mathbf{s}$ is the vector in reciprocal space ($s = 2/\lambda \sin\theta$, Bragg angle $\theta$, wavelength $\lambda$), $I_l(\mathbf{s})$ is the scattering intensity of a lamellar structure, and $\mathbf{T}_i$ is a tensor of rotation defining the orientation of the lamellar structure $i$ with respect to the sample-fixed coordinates.

$$I_l(\mathbf{s}) = |\Phi_D|^2 (s_{12})\, I_1(s_3) = I_l(s_{12}, s_3)$$

$\Phi_D$ is the Fourier transform of the shape factor defining the lateral extension of the lamellae, $I_1$ is the 1D scattering function of the lamellar stacking, $s_1$, $s_2$, and $s_3$ are components of $\mathbf{s}$ in a rectangular system of coordinates, $s_3$ is directed parallel to the principal axis, and $s_{12} = (s_1^2 + s_2^2)^{1/2}$. Since both $I(\mathbf{s})$ and $I_l(\mathbf{s})$ are cylindrically symmetrical, i.e., $s_{12} = s \sin\phi$, $s_3 = s \cos\phi$, the orientation of the lamella normals can be introduced by the series development

$$I(s, \phi) = \sum_{n=0}^{\infty} \alpha_{2n}(s)\, P_{2n}(\cos\phi_0)\, P_{2n}(\cos\phi) \qquad (1)$$

where $\phi$ is the polar angle, $\phi_0$ is the main direction of the lamella normals, and $P_{2n}(z)$ are Legendre polynomials. The coefficients $a_{2n}(s)$ are defined by

$$I_0(s, \phi) = \sum_{n=0}^{\infty} a_{2n}(s)\, P_{2n}(\cos\phi) \qquad (2)$$

$I_0(s, \phi)$ represents the distribution obtainable if $\phi_0 = 0$. It is composed of $I_l(s, \phi)$ and the orientation distribution $g(\phi)$ about $\phi_0$. If we assume the lateral extension of the lamellae to be much larger than the periodicity of the stacking, we can use the approximations $s_{12} \simeq s\phi$ and $s_3 \simeq s$, i.e.

$$I_l(s, \phi) \simeq |\Phi_D|^2 (s\phi)\, I_1(s)$$

For constant $s$, the integral width of $I_0(s, \phi)$ in $\phi$, $B_0(s)$, can be approximated by the relationship

$$s^2 B_0^2(s) \propto s^2 B_g^2 + D^{-2} \qquad (3)$$

where $B_g$ is the integral width of $g(\phi)$ and $D$ is the average lateral extension of the lamellae. For $I_0(s, 0)$ we find the approximation

$$I_0(s, 0) \propto \frac{I_1(s)}{s^2 B_g^2 + D^{-2}} \qquad (4)$$

By appropriate methods of evaluation, we can extract from $I_l(s, \phi)$ the structural parameters $\phi_0$, $B_g$, and $D$ as well as the 1D scattering function $I_1(s)$. The latter can be used to obtain parameters defining the stacking of the lamellae, notably the two average thicknesses $\overline{d_1}$ and $\overline{d_2}$, the average period $\overline{L} = \overline{d_1} + \overline{d_2}$, and the volume concentrations $c_i = \overline{d_i}/\overline{L}$. The evaluation of $I_1(s)$ can be carried out by calculation of the interface distribution function (IDF)[15,17] or by fitting of theoretical $I_1(s)$ curves to experimental ones. In the latter case two standard models are in general use, the stack model[18]

$$s^2 I_1(s) \propto \mathrm{Re}\, \frac{[1 - H_1(s)][1 - H_2(s)]}{1 - H_1(s)\, H_2(s)} \qquad (5)$$

and the lattice model[19]

$$s^2 I_1(s) \propto 1 - \mathrm{Re}[H_1(s)] + 4\, \mathrm{Im}\,[H_1(s/2)]^2\, \mathrm{Re}\left[\frac{H_L(s)}{1 - H_L(s)}\right]$$

where Re and Im stand for real and imaginary part, respectively, and $H_1$, $H_2$, and $H_L$ are the Fourier transforms of the distributions of $d_1$, $d_2$, and $L$, respectively, of the type

$$Hj(s) = \exp(2\pi i \overline{d_j} s - 2\pi^2 \sigma_j^2 s^2)$$

where $\sigma_j^2$ is the variance of $d_j$. A recent example of this application is given by Wolff, Burger, and Ruland.[20]

**2.2. Microvoids.** The scattering intensity of a dilute system of elongated microvoids with preferred orientation can be treated similarly to that of lamellar structures given above. The intensity distribution $I_v$ of a single microvoid of cylindrical shape oriented with the principal axis parallel to $s_3$ can be approximated by

$$I_v(s_{12}, s_3) = |\Phi_{12}|^2 (s_{12})\, |\Phi_3|^2 (s_3)$$

$\Phi_{12}$ and $\Phi_3$ are the Fourier transforms of the shape functions defining the extensions $L_{12}$ and $L_3$ of the microvoid in the direction of $s_{12}$ and $s_3$, respectively. If $L_{12} \ll L_3$, $I_v$ has the shape of a flat disk. The scattering of an ensemble of microvoids with the main orientation in the direction of $s_3$ is represented by a fan-shaped intensity distribution in the planar section containing $s_3$.[12] In the present paper, we are only interested in the contribution of the microvoid scattering to the scattering of the lamellae in the direction of $\phi = 0$. This can be approximated for $s > 1/L_3$ by

$$I_v(s, 0) \propto [s^2 (1 + 4\pi^2 L_3^2 s^2)]^{-1} \qquad (6)$$

In this paper, eq 6 is used only as an approximation for the background scattering in the meridional SAXS. A more detailed SAXS study of the microvoid formation in PAN fibers will be published in a separate paper.[13]

## 3. Experimental Section

The first type of PAN fibers investigated was a PAN homopolymer (<0.7% methyl acrylate) produced by Hoechst (Dolanit). The homopolymer fibers have initial tensile moduli of about 17 GPa, extensions at a break of about 8%, and diameters of about 16 $\mu$m. The second type was a PAN copolymer fiber produced by Sigri as a precursor for carbon fibers. It contains 2−6% methyl acrylate as well as itaconic acid. The copolymer fibers have initial tensile moduli of about 11 GPa, extensions at a break of 17%, and diameters of about 14 $\mu$m. Time-resolved SAXS measurements were performed at DESY in Hamburg, Germany. The combination of synchrotron radiation ($\lambda = 0.150$ nm, pinhole collimation) and 1D as well as 2D position-sensitive detectors was used to follow the

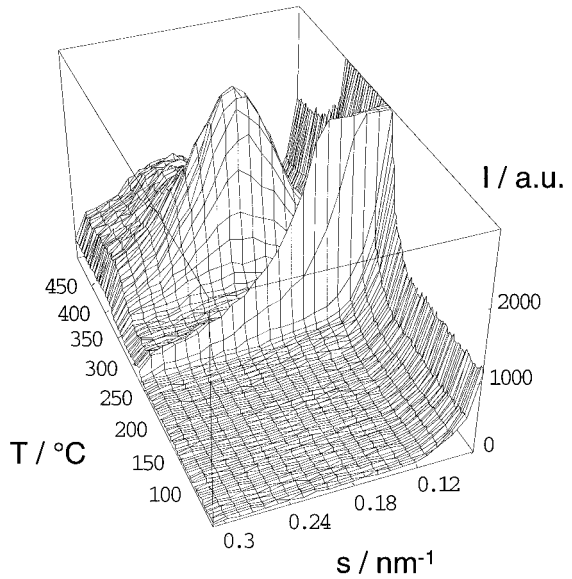


**Figure 2.** Temperature-dependent meridional SAXS of PAN homopolymer fibers. The heating rate is 13 K/min.

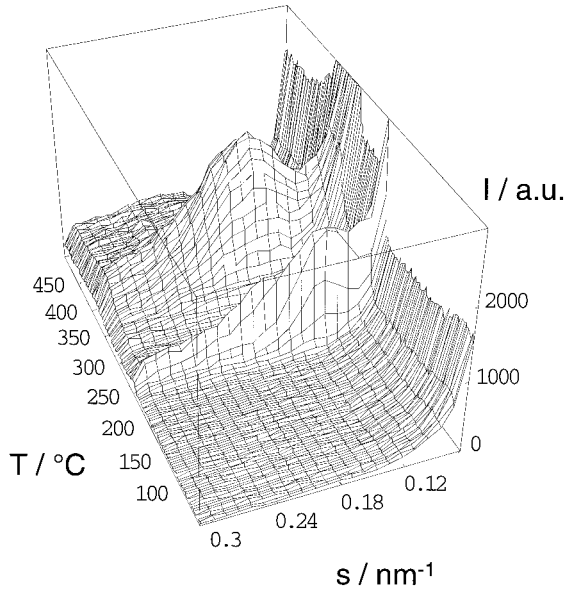


**Figure 3.** Temperature-dependent meridional SAXS of PAN copolymer fibers. The heating rate is 13 K/min.

kinetics of the mesophase formation as a function of time and temperature.

## 4. Results and Discussion

No scattering maxima were observed in the SAXS diagrams of both the homopolymer and the copolymer PAN fibers; only a weak equatorial scattering due to microvoids was visible. This indicates that no lamellar systems are present in the pristine fibers, corroborating the results of the earlier studies on PAN fibers[14] in which a homogeneously disordered structure with predominantly extended chains was found.

**4.1. Formation of Lamellar Mesophases.** Typical temperature-dependent meridional scattering curves of homopolymer and copolymer fibers are shown in Figures 2 and 3. In both cases we observe the appearance and disappearance of two distinctly different meridional maxima indicating the formation and destruction of two different types of lamellar mesophases. The first maximum appears in a relatively narrow temperature range

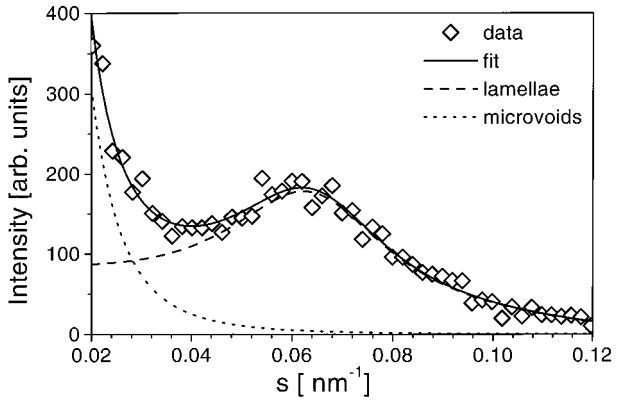


**Figure 4.** Meridional SAXS of the α phase of a PAN copolymer fiber. The diamonds represent the experimental values at 295 °C; the solid line is the fit of a superposition of eqs 5 and 6. The dashed line is the scattering component of the lamellae; the dotted line is the scattering component of the microvoids. The heating rate is 13 K/min.

between 220 and 310 °C, depending on the heating rate. The second maximum appears in a somewhat larger temperature range beginning at about 350 °C. We designate the maxima and the corresponding phases by α and $\beta$. We assume that the α phase is formed during the cyclization and the $\beta$ phase during the aromatization (see Figure 1). The α phase is represented by a lamellar system composed of pristine and cyclized PAN chain segments, and the $\beta$ phase by cyclized and aromatized PAN chain segments. In the temperature ranges before the appearance of the α maximum, between the α and the $\beta$ maximum and after the $\beta$ maximum, the fiber structure is homogeneous except for the SAXS of microvoids. It was observed that the cyclization, which is a strongly exothermic process, was completed at the temperature range between the α and the $\beta$ phase, as indicated by the absence of an exothermic response in differential scanning calorimetry.

The maximum corresponding to the α phase was mentioned earlier in the literature[6,8,10,11,21] and was interpreted in analogy to the SAXS of rayon fibers[12] as resulting from a self-contrasting two-phase system.[10,21] This interpretation presumes the existence of a lamellar two-phase system in the pristine fibers, such as a semicrystalline structure. However, the earlier work on PAN fibers[14] has definitely shown that such structures are absent. Therefore, another explanation for the formation of the α phase has to be found.

**4.2. Structural Parameters.** For a quantitative description of the α and $\beta$ phase, we used two independent evaluation methods. The first is based on curve fitting using eqs 5 and 6 (see Figures 4 and 5), and the second used the calculation of the interface distribution function[15,17] (see Figures 6 and 7), which is an established method for the description of lamellar mesophase systems, for example, block copolymers,[20,22] semicrystalline polymers,[23] and polyelectrolyte−surfactant complexes.[24] The results of both methods gave equivalent results, which are shown in Tables 1 and 2.

An inspection of the tables shows that the average periods of the α phase (≃13 nm) and the $\beta$ phase (≃5 nm) are sufficiently different to exclude a common origin of the periodicity, especially since the shrinkage of the fibers is about 10% at maximum.

The interpretation of the values given for $c_1$ (and, consequently, for $\bar{d}_1$) has to be considered with care. These values have been obtained with the assumption

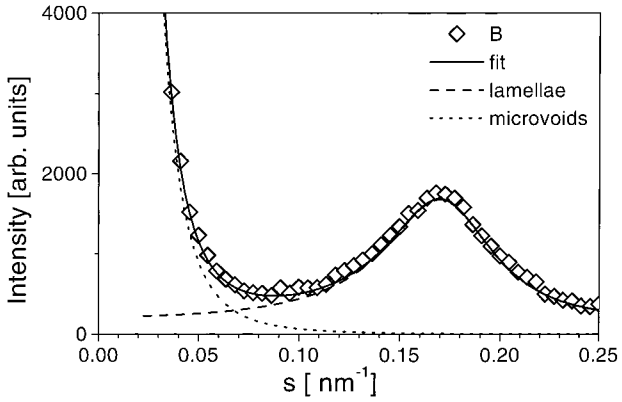


**Figure 5.** Meridional SAXS of the $\beta$ phase of a PAN homopolymer fiber at 400 °C (diamonds) and the fit according to the sum of eqs 5 and 6 (solid line). The dashed line represents the contribution of the lamellar phase, and the dotted line represents the contribution of the microvoids.

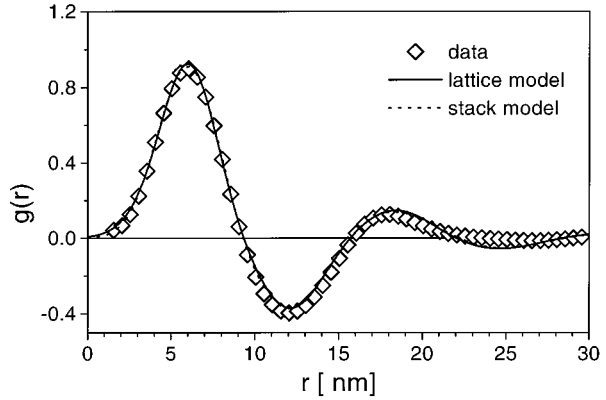


**Figure 6.** Interface distribution function of the α phase of a copolymer fiber (diamonds) and fits according to the lattice model (solid line) and the stack model (dashed line). The temperature is 285 °C.

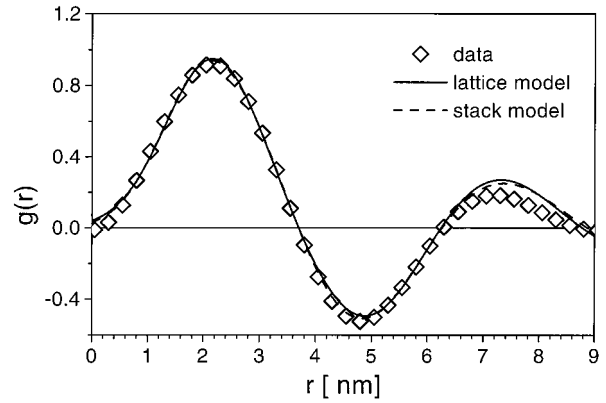


**Figure 7.** Interface distribution function of the $\beta$ phase of a copolymer fiber (diamonds) and fits according to the lattice model (solid line) and the stack model (dashed line). The temperature is 400 °C.

of a uniform concentration of the phase of type 1 throughout the sample during the cyclization and the aromatization reaction. This uniformity is, however, very unlikely to exist during pyrolytic reactions. It is resonable to assume that, for a given average spacing $\bar{L}$, a distribution of concentrations is present in the sample. Furthermore, the scattering curves have been measured within a finite time interval, which results in a supplementary nonuniformity. The effect of a concentration distribution on scattering curves as given by eq 5 has been studied. It was found that, in the range of $s$ values used for the fitting procedure shown in Figures 4 and 5, there is little difference between a curve based on a uniform concentration of a given value $c_1$ and a distribution of concentrations centered on $c_1 = 0.5$ with a given width $\Delta c$. The latter is obtained by

$$\langle I_1(s)\rangle \propto \frac{1}{\Delta c}\int_{(1-\Delta c)/2}^{(1+\Delta c)/2} I_1(s, c_1)\, \mathrm{d}c_1$$

where $I_1(s, c_1)$ is the scattering curve of a lamellar structure according to eq 5 with constant values of $\bar{L} = \bar{d}_1 + \bar{d}_2$ and $\sigma_i$ but varying values of $c_1 = \bar{d}_1/\bar{L}$. We found that, in the range of $s$ values used for the curve fitting ($0.3/\bar{L} \lesssim s \lesssim 2/\bar{L}$), $\langle I_1(s)\rangle$ curves can be calculated that are very similar to $I_1(s, c_1)$ curves, and that the relationship between $c_1$ and $\Delta c$ is, to a first approximation, given by

$$\Delta c \simeq \sqrt{3}\,|1 - 2c_1|$$

in the range $0.25 < c_1 < 0.75$. Consequently, the values of $c_1$ shown in the last column of Tables 1 and 2 can be interpreted in terms of the corresponding widths $\Delta c$ of concentration distributions centered on $c = 0.5$. For example, a uniform concentration of $c_1 = 0.36$ would correspond to an average concentration of 0.5 with $\Delta c = 0.48$. The latter interpretation appears to be more reasonable in view of the expected nonuniformity of the concentrations.

The orientation parameters $\phi_0$ and $B_g$ as well as the lateral dimension $D$ of the lamellar stacks were determined using eq 3. An example of a $s^2B_0$ versus $s^2$ plot is given in Figure 8. The average tilt angle $\phi_0$ between the fiber axis and the lamella normals was about ±15° for both the α and the $\beta$ phase. For the α phase, $B_g$ is about 33° as already observed by Burger and Ruland;[25] for the $\beta$ phase $B_g$ was found to be much wider (≈90°). The α phase shows values of $D$ in the range 50−100 nm,[25] whereas the $D$ values for the $\beta$ phase are much lower (≈15 nm).

**Table 1. Structural Parameters of the α Phase Measured at Constant Temperatures**[a]

| sample | $T$ (°C) | $\bar{d}_1$ (nm) | $\bar{L}$ (nm) | $c_1$ |
|---|---|---|---|---|
| C | 230 | 2.9 | 8.3 | 0.35 |
| C | 250 | 4.3 | 10.3 | 0.42 |
| C | 280 | 6.1 | 13.5 | 0.45 |
| C | 285 | 5.6 | 12.7 | 0.44 |
| C | 295 | 4.9 | 13.8 | 0.36 |
| H | 285 | 2.9 | 12.7 | 0.23 |
| H | 295 | 5.1 | 14.2 | 0.36 |
| H | 300 | 4.4 | 13.9 | 0.32 |

[a] H, homopolymer; C, copolymer; $\bar{d}_1$, average thickness of the lamellae of type 1; $\bar{L} = \bar{d}_1 + \bar{d}_2$, average period of the lamellar system; $c_1 = \bar{d}_1/\bar{L}$, volume concentration of lamellae of type 1.

**Table 2. Structural Parameters of the $\beta$ Phase Measured at 400 °C as a Function of the Heating Rate d$T$/d$t$ To Reach This Temperature**[a]

| sample | d$T$/d$t$ (K/min) | $\bar{d}_1$ (nm) | $\bar{L}$ (nm) | $c_1$ |
|---|---|---|---|---|
| C | 13 | 1.5 | 5.0 | 0.30 |
| C | 30 | 2.0 | 5.1 | 0.39 |
| C | 60 | 1.5 | 4.8 | 0.31 |
| H | 13 | 2.0 | 5.5 | 0.36 |
| H | 30 | 1.8 | 5.4 | 0.33 |
| H | 60 | 1.8 | 5.5 | 0.33 |

[a] H, homopolymer; C, copolymer; $\bar{d}_1$, average thickness of the lamellae of type 1; $\bar{L} = \bar{d}_1 + \bar{d}_2$, average period of the lamellar system; $c_1 = \bar{d}_1/\bar{L}$, volume concentration of lamellae of type 1.

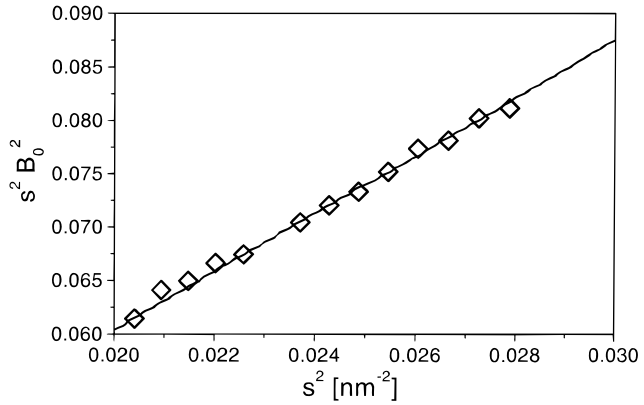


**Figure 8.** Plot of $s^2B_0^2$ versus $s^2$ of the tangential intensity distribution of the $\beta$ phase.

The most probable explanation for the tilt angle $\phi_0$ is the formation of a morphology similar to pleated-sheet structure, comparable to that observed in PPTA fibers,[26] during the thermal relaxation of the PAN fibers. It should, however, be noted that the final morphology of PAN-based carbon fibers does not show a pleated-sheet structure, in contrast to carbon fibers produced from mesophase pitch.[27]

**4.3. Kinetics of Formation.** To study the kinetics of formation of the lamellar mesophases, we used the total SAXS scattering $k$ (Porod invariant) as a parameter. In cylindrically symmetrical systems, $k$ is given by

$$k = 4\pi \int_0^\infty \int_0^\infty s_{12}\, I(s_{12}, s_3)\, \mathrm{d}s_{12}\, \mathrm{d}s_3$$

$$= 2\pi \int_0^\infty \int_0^{\pi/2} sI(s, \phi) \sin\phi\, \mathrm{d}\phi\, \mathrm{d}s$$

$$= V\,(\rho_1 - \rho_2)^2\, c(1 - c)$$

where $V$ is the total irradiated volume, $\rho_i$ is the electron density of the lamellae of type $i$, and $c$ is the volume concentration of one type of lamellae. Since we are not measuring absolute intensities, the experimental values of $k$ are proportional to $(\rho_1 - \rho_2)^2\, c(1 - c)$ provided that $V$ is kept constant, i.e., that there is no significant loss of material in the irradiated volume during the measurements. Separate measurements have shown that the weight loss of the fibers has been about 5% in the temperature and time range used. In calculating $k$ from the 2D intensity distributions, care was taken to exclude the equatorial scattering due to microvoids.

Figure 9 shows plots of $k$ for the homopolar fiber as a function of temperature for various heating rates; Figure 10 shows a similar plot for the copolymer fiber. The formation of the α and $\beta$ phase results in characteristic maxima of the temperature dependence of $k$. At a heating rate of 6 K/min, we found that the maximum of the α phase of the homopolymer fibers is located at 270 °C, whereas that of the copolymer fibers is at about 250 °C. At a heating rate of 20 K/min, the corresponding temperatures are 310 and 270 °C, respectively. This difference can be explained by the catalytic effect of the comonomers on the formation of the α phase. For the $\beta$ phase, the situation is not clear. At a heating rate of 6 K/min, the maxima are located at about 385 °C for both fibers, whereas at a heating rate of 20 K/min, the positions of the maxima differ markedly: 435 °C for the homopolymer, 400 °C for the copolymer fiber.

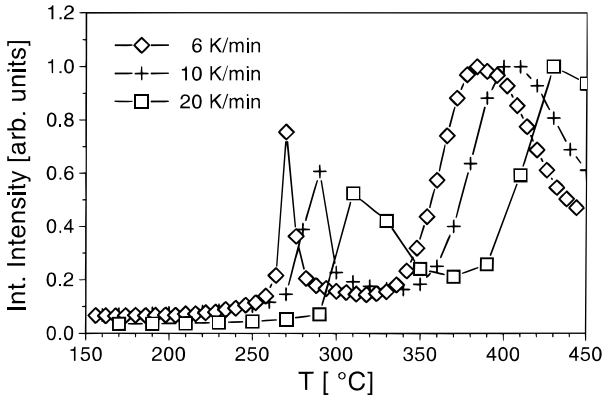


**Figure 9.** Temperature dependence of the integral SAXS of PAN homopolymer fibers determined from 2D scattering patterns. The heating rates are 6 K/min (diamonds), 10 K/min (crosses), and 20 K/min (squares).

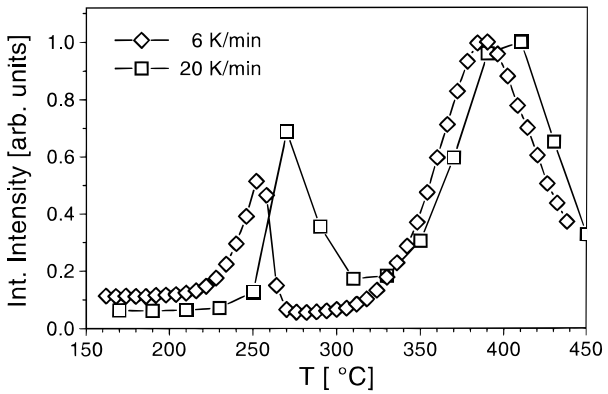


**Figure 10.** Temperature dependence of the integral SAXS of PAN copolymer fibers determined from 2D scattering patterns. The heating rates are 6 K/min (diamonds) and 20 K/min (squares).

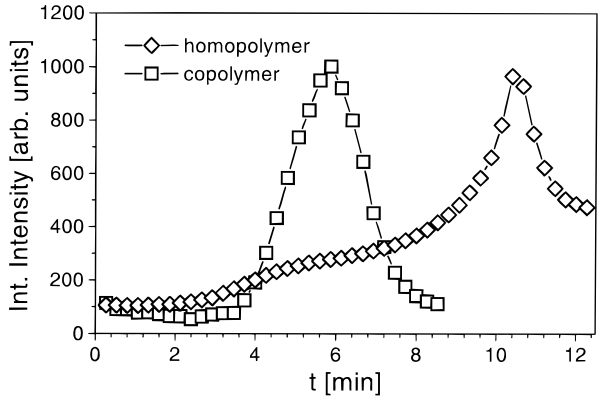


**Figure 11.** Time dependence of the integral SAXS of homo- and copolymer fibers. The temperature is held constant at 285 °C.

Figure 11 shows the development of the α phase as a function of time at constant temperature (285 °C). The homopolymer fiber shows a maximum at about 5.8 min, whereas the copolymer fiber shows a flat maximum at about 4.8 min followed by a sharp maximum at about 10.5 min.

## 5. Conclusions

The results of the present study can be summarized as follows:

1. The cyclization and the aromatization of PAN fibers proceed in well-separated steps, which are characterized

by the appearance of two types of lamellar mesophases that we call α and $\beta$, respectively.

2. The α phase appears in the temperature range from about 200 to 300 °C. It shows a period of about 13 nm. The lamellae are composed of pristine and cyclized PAN chain segments. The kinetics of formation depends on the temperature and the composition of the fiber.

3. The $\beta$ phase appears at temperatures higher than about 350 °C. It shows a period of about 5 nm. The lamellae are composed of cyclized and aromatized PAN chain segments.

4. Homopolymer and copolymer fibers differ considerably in the kinetics of developing the α phase.

5. The formation of the phases cannot be explained by a self-contrasting process of a lamellar structure already existing in the pristine fibers.

6. Both phases show a tilt angle of about 15° of the lamella normals with respect to the fiber axis. The origin of this orientation is probably a pleated-sheet structure developing during the thermal relaxation of the fibers.

**Acknowledgment.** We thank Dr. Fester (Hoechst AG) for providing the PAN fibers and Dr. R. Zietz for helpful assistance with the synchrotron SAXS measurements.

## References and Notes

(1) Wöhrle, D. *Adv. Polym. Sci.* **1977**, *10*.
(2) Olivé, G. H.; Olivé, S. *Adv. Polym. Sci.* **1983**, *51*.
(3) Jain, M. K.; Abhiraman, A. S. *J. Mater. Sci.* **1987**, *22*, 278.
(4) Jain, M. K.; Balasubramanian, M.; Desai, P.; Abhiraman, A. S. *J. Mater. Sci.* **1987**, *22*, 278.
(5) Bashier, Z. *Carbon* **1991**, *29*, 1081.
(6) Tyson, C. N. *Nat. Phys. Sci.* **1971**, *229*, 121.
(7) Fillery, M. E.; Goodhew, P. J. *Nat. Phys. Sci.* **1971**, *233*, 118.
(8) Hinrichsen, G. *J. Appl. Polym. Sci.* **1973**, *17*, 3305.
(9) Warner, S. B. *J. Polym. Sci., Polym. Lett.* **1978**, *16*, 287.
(10) Warner, S. B.; Uhlmann, D. R.; Peebles, L. H. *J. Mater. Sci.* **1979**, *14*, 1893.
(11) Walenta, E.; Fink, H. P. *Acta Polym.* **1990**, *40*, 598.
(12) Ruland, W. *J. Polym. Sci., Part C* **1969**, *28*, 143.
(13) Thünemann, A. F.; Ruland, W., in press.
(14) Liu, X. D.; Ruland, W. *Macromolecules* **1993**, *26*, 3030.
(15) Ruland, W. *Colloid Polym. Sci.* **1977**, *255*, 833.
(16) Ruland, W. *Colloid Polym. Sci.* **1977**, *255*, 417.
(17) Ruland, W. *Colloid Polym. Sci.* **1978**, *256*, 923.
(18) Hermans, J. J. *Recl. Trav. Chim. Pays-Bas* **1944**, *63*, 311.
(19) Tsvankin, D. Y.; Zubov, A. Y.; Kitaigorodskii, A. I. *J. Polym. Sci.* **1968**, *C16*, 4081.
(20) Wolff, T.; Burger, C.; Ruland, W. *Macromolecules* **1994**, *27*, 3301.
(21) Hinrichsen, G.; Orth, H. *Kolloid-Z.* **1971**, *247*, 844.
(22) Stribeck, N.; Reimers, C.; Chioca, P.; Buzdugan, E. J. *Polym. Sci., Part B: Polym. Phys.* **1998**, *36*, 1423.
(23) Stribeck, N.; Zachmann, H. G.; Bayer, R. K.; Calleja, F. J. B. *J. Mater. Sci.* **1997**, *32*, 1639.
(24) Thünemann, A. F.; Lochhaas, K. H. *Langmuir* **1998**, *14*, 6220.
(25) Burger, C.; Ruland, W. *Extended Abstracts of the 20th Biennial Conference on Carbon, Santa Barbara*, 1991; p 276.
(26) Dobb, M. G.; Johnson, D. J.; Saville. *J. Polym. Sci., Polym. Symp.* **1977**, *58*, 237.
(27) Yoon, S. H.; Korai, Y.; Mochida, I. *Carbon* **1994**, *32*, 1182.

MA991298K